

Some developments in constitutive modelling of soft clays

S.J. Wheeler
University of Glasgow, UK

M. Cudny, H.P. Neher
University of Stuttgart, Germany

C. Wiltafsky
Graz University of Technology, Austria

ABSTRACT: The paper summarises recent developments in constitutive modelling of soft clays achieved by members of the SCMEP Research Training Network. The work has focused on the modelling of anisotropy of large strain behaviour, destructuration and creep/time-dependency. Two alternative approaches have been used for representing anisotropy of plastic behaviour: elasto-plastic models with a rotational component of hardening and the multilaminate framework. These two approaches have both been used in models which also incorporate the influence of inter-particle bonding and destructuration. Elasto-viscoplasticity has been used for the modelling of creep and time-dependency, including a multilaminate model which also represents anisotropy of large strain behaviour. The constitutive models provide improved modelling of the stress-strain behaviour of natural soft clays, leading to enhanced capabilities for numerical analysis of construction activities in soft clays.

1 INTRODUCTION

A Research Training Network on Soft Clay Modelling for Engineering Practice (SCMEP) has been funded by the European Community for a 4 year period (2000-2004). The Network involves 5 teams at the University of Glasgow (UK), Helsinki University of Technology (Finland), the University of Stuttgart (Germany), Graz University of Technology (Austria) and the Norwegian University of Science and Technology, Trondheim (Norway). The research tasks of the Network were grouped under 3 main headings of constitutive modelling, numerical implementation and practical application. This paper summarizes the main developments in constitutive modelling achieved in the first 3 years of the Network.

The work of the Network on constitutive modelling focused on 3 main issues: anisotropy, destructuration and time-dependency/creep. Improved models were to be developed incorporating the influence of these three factors, including two or more factors in combination. Modelling developments were to be validated by experimental data from laboratory test programmes undertaken by the Network teams or by experimental data from the literature. The aim was not to produce a single constitutive model, but to explore alternative strategies and models for representing a given phenomenon. These alternatives could then be compared against each other and against experimental data, so that the successes and limitations of different modelling approaches could be identified.

The constitutive models were to be subsequently implemented in commercially available finite element programs and then applied (together with more conventional constitutive models) in the numerical analysis of both fictitious benchmark boundary value problems and real case histories, including embankments, excavations and tunnels. The intention was to demonstrate the improved modelling capabilities and the practical implications for analysis and design of geotechnical construction in soft clays. These aspects of numerical implementation and application are not covered in this paper.

If widespread practical application of the constitutive models was to be a realistic hope for the future, they had to be kept as simple as possible commensurate with realistic modelling of the mechanical behaviour of natural soft clays. This meant that aspects of soil behaviour that were considered relatively unimportant in the case of soft clays were to be excluded from the models (rather than attempting to develop more generalized models that could be applied to any category of clay or even any class of soil). It was also important that model parameters could be measured reasonably simply, preferably in relatively standard laboratory tests. A crucial factor was that the models should be as easy to understand as possible, because use of a model will always remain limited if proper understanding of the model is restricted to a small number of individuals.

2 ANISOTROPY

Natural soft clays tend to have significant anisotropy of fabric, developed during deposition and one-dimensional consolidation. During subsequent straining, re-orientation of particles and changes in particle contacts can lead to changes in the anisotropy.

Fabric anisotropy can influence both elastic behaviour and plastic behaviour. For normally consolidated or lightly overconsolidated soft clays, however, plastic deformations are likely to dominate for many problems of practical interest, with elastic strains often being relatively unimportant. Attention therefore concentrated on modelling of plastic anisotropy.

Two different approaches for constitutive modelling of anisotropy of plastic behaviour have been investigated by the Network teams. Work at Glasgow and Helsinki has focused on use of elasto-plastic models with a rotational component of hardening, whereas the teams at Graz and Stuttgart have worked on use of the multilaminate framework.

2.1 *Rotational hardening model S-CLAY1*

The anisotropic elasto-plastic model S-CLAY1, developed at Glasgow and Helsinki, is an extension of conventional critical state models, with anisotropy of plastic behaviour represented through an inclined yield surface and a rotational component of hardening to model the development or erasure of fabric anisotropy during plastic straining. An initial version of the model was proposed by Wheeler (1997) and this was subsequently modified to its current form by Näätänen, Wheeler, Karstunen & Lojander (1999) and Wheeler, Näätänen, Karstunen & Lojander (2003).

For the simplified conditions of a triaxial test on a cross-anisotropic sample, with the horizontal plane in the triaxial sample coinciding with the plane of isotropy of the sample, the S-CLAY1 yield curve can be expressed in terms of the mean effective stress p' and deviator q :

$$f = (q - \alpha p')^2 - (M^2 - \alpha^2)(p'_m - p')p' = 0 \quad (1)$$

where M is the value of the stress ratio $\eta=q/p'$ at critical states, p'_m defines the size of the yield curve and α defines the orientation of the yield curve (see Fig. 1a). The yield curve is in the form of a sheared ellipse, and is identical to that suggested by Dafalias (1987) and Korhonen & Lojander (1987). The scalar parameter α is a measure of the degree of plastic anisotropy of the soil. With $\alpha=0$ the soil behaviour is isotropic and Eq. 1 corresponds to the yield curve in the conventional Modified Cam Clay model (Roscoe & Burland (1968)).

Wheeler, Karstunen & Näätänen (1999) and Wheeler, Näätänen, Karstunen & Lojander (2003) showed how the initial value of the parameter α can be determined (simply through knowledge of the friction angle ϕ' of the soil) for a clay deposit with a history of one-dimensional straining to a

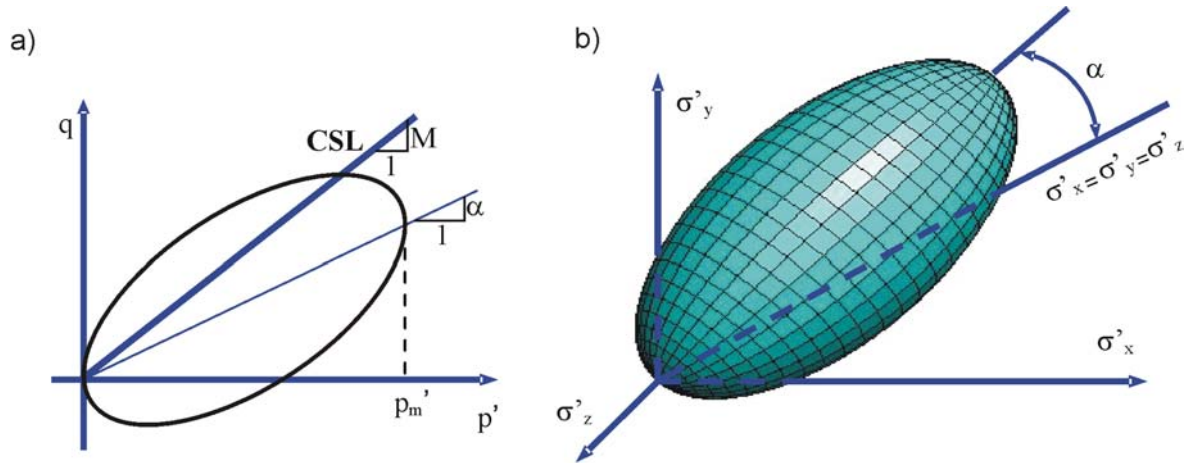


Figure 1. SCLAY1S yield surface a) in triaxial stress space b) 3-D stress space

normally consolidated or lightly overconsolidated state. Wheeler, Näätänen, Karstunen & Lojander (2003) showed that the yield curve shape of Eq. 1 (including the procedure recommended for establishing the initial value of α) provided a good match to the initial shape of the yield curve identified from experimental tests on undisturbed samples of Otaniemi clay, a soft clay from southern Finland. They also showed good matches for 4 other soft clays reported by Diaz-Rodriguez, Leroueil & Aleman (1992), while Näätänen & Lojander (2000) showed similar agreement for 4 further Finnish clays.

A generalized version of the yield surface is required for numerical analysis of boundary value problems, where three-dimensional stress states and rotation of principal stress directions occur:

$$f = \frac{3}{2} \left[\{\underline{\sigma}_d - p' \underline{\alpha}_d\}^T \{\underline{\sigma}_d - p' \underline{\alpha}_d\} \right] - \left[M^2 - \frac{3}{2} \{\underline{\alpha}_d\}^T \{\underline{\alpha}_d\} \right] (p'_m - p') p' = 0 \quad (2)$$

where $\underline{\sigma}_d$ is the deviatoric stress tensor and $\underline{\alpha}_d$ is a deviatoric fabric tensor (see Wheeler, Näätänen, Karstunen & Lojander (2003) and Zentar, Karstunen, Wheeler & Näätänen (in press)). Eq. 2 shows that the generalized version of the yield surface cannot be expressed solely in terms of stress invariants. Fig. 1b shows the form of the S-CLAY1 yield surface in three-dimensional stress space, for the case where the principal axes of both the stress tensor and the fabric tensor coincide with the x, y and z directions.

The S-CLAY1 model assumes isotropic elastic behaviour (of the same form as in Modified Cam Clay) and an associated flow rule.

S-CLAY1 incorporates two hardening laws. The first describes change of size of the yield surface, which is assumed to be related solely to the increments of plastic volumetric strain $d\varepsilon_v^p$ (as in Modified Cam Clay) :

$$dp'_m = \frac{vp'_m d\varepsilon_v^p}{\lambda - \kappa} \quad (3)$$

where v is the specific volume, κ is the gradient of elastic (pre-yield) swelling lines in the $v:\ln(p')$ plane and λ is the gradient of the post-yield compression curve in the $v:\ln(p')$ plane for a constant η stress path involving no change of anisotropy ($\alpha=\text{constant}$), such as isotropic loading of an isotropic sample.

The second hardening law (the “rotational hardening law”) describes the change of orientation of the yield surface with plastic straining. For the simplified conditions of a triaxial test on a co-axial cross-anisotropic sample, this rotational hardening law takes the form:

$$d\alpha = \mu \left(\left[\frac{3\eta}{4} - \alpha \right] \langle d\varepsilon_v^p \rangle + \beta \left[\frac{\eta}{3} - \alpha \right] |d\varepsilon_d^p| \right) \quad (4)$$

where $d\varepsilon_d^p$ is the increment of plastic deviatoric strain and μ and β are two additional soil constants. Inspection of Eq. 4 shows that, in the model, positive plastic volumetric strains attempt to drag α towards an instantaneous target value of $3\eta/4$, whereas plastic shear strains (whether positive or negative) attempt to drag α towards a different instantaneous target value of $\eta/3$. The soil constant β controls the relative effectiveness of plastic shear strains and plastic volumetric strains in setting the overall instantaneous target value for α (which will lie between $3\eta/4$ and $\eta/3$), whereas the soil constant μ controls the absolute rate of rotation of the yield surface towards its current target value of α . Wheeler, Karstunen & Näätänen (1999) and Wheeler, Näätänen, Karstunen & Lojander (2003) presented procedures for determining the values of the soil constants μ and β . The generalized version of Eq. 4, appropriate to three-dimensional stress states, including the possibility of rotation of principal stress directions and non-coaxiality of stress and fabric tensors, is given by Wheeler, Näätänen, Karstunen & Lojander (2003) and Zentar, Karstunen, Wheeler & Näätänen (in press) as:

$$d\underline{\alpha}_d = \mu \left(\left[\frac{3\eta}{4} - \underline{\alpha}_d \right] \langle d\varepsilon_v^p \rangle + \beta \left[\frac{\eta}{3} - \underline{\alpha}_d \right] |d\varepsilon_d^p| \right) \quad (5)$$

where $\underline{\eta} = \underline{\alpha}_d / p'$.

The rotational hardening law of Eq. 4 was developed and validated on the basis of a substantial programme of experimental tests on Otaniemi clay (Näätänen, Wheeler, Karstunen & Lojander (1999); Wheeler, Näätänen, Karstunen & Lojander (2003)). Each test involved a first loading stage, at a constant value of η , to a stress 2-3 times larger than the yield value. This was followed by unloading and then a second loading stage, at a different value of η . The objectives were to find not only a series of yield points from the first loading stages defining the initial size and orientation of the yield curve, but also to load each sample far enough during the first stage to get some rotational hardening and to subsequently identify a point on the expanded and rotated yield curve during the second loading stage. The rotational hardening laws proposed by most previous authors had not been validated by this form of comprehensive purpose-designed experimental investigation. Further support for the rotational hardening law of Eq. 4 was subsequently provided by similar test programmes on other natural and reconstituted soft clays, including POKO clay from Finland (Koskinen, Zentar & Karstunen (2002) ; Koskinen, Karstunen & Wheeler (2002)), Bothkennar clay from Scotland (McGinty, Karstunen & Wheeler (2001)) and other Finnish clays (not yet published).

The rotational hardening law of Eq. 4 (or the generalized version given in Eq. 5) includes explicit dependence on both plastic volumetric strains and plastic shear strains. This feature is also found in the anisotropic model of Pestana & Whittle (1999). In contrast, in many other proposed anisotropic models the rotational hardening law depends solely on plastic volumetric strains (see, for example, Banerjee & Yousif (1986), Dafalias (1987), Davies & Newson (1993) and Whittle & Kavvas (1994)) or solely on plastic shear strains (see, for example, Yu & Axelsson (1994)), which is physically unreasonable and can result in illogical predictions for certain stress paths (see Karstunen & Wheeler (2002)).

S-CLAY1 model simulations of tests on reconstituted samples of POKO clay anisotropically consolidated with a K_0 stress history, showed excellent agreement with the behaviour observed in laboratory tests (Koskinen, Zentar & Karstunen (2002)). The tests included loading under a full range of η values, with each test involving first and second loading stages at different values of η . Subsequent simulations of similar test programmes on reconstituted samples of 3 other Finnish clays (Otaniemi, Murro and Vanttila) also show excellent agreement (not yet published). These successful simulations demonstrate the accuracy of the yield curve shape (Eq. 1), the hardening laws (Eqs. 3 and 4) and the associated flow rule, when applied to reconstituted soft clays.

S-CLAY1 simulations of tests on natural soft clays were less successful. Although values of yield stress were generally well-predicted in all test stages, providing support for the yield curve shape (Eq. 1) and the rotational hardening law (Eq. 4), it was impossible to correctly match the plastic volumetric strains observed in all test stages. If the value of λ was selected to match the post-yield volumetric strains observed in test stages performed at low value of η , then post-yield volumetric strains were substantially under-predicted in test stages performed at high values of η (Wheeler, Karstunen & Näätänen (1999), Wheeler, Näätänen, Karstunen & Lojander (2003)). This was attributed to the influence of destructuration, with destructuration progressing at different rates in test stages performed at different values of η . This highlighted the importance of incorporating destructuration as well as anisotropy in constitutive models intended for use with natural soft clays (see Section 3 below).

Experience with performing model simulations of laboratory tests emphasized the importance of using appropriate procedures for identifying yield points from experimental stress-strain curves. An anisotropic model, such as S-CLAY1, predicts considerable curvature of the post-yield compression curve of volumetric strain ε_v plotted against $\ln(p')$ if rotation of the yield curve is occurring i.e. if the anisotropy is changing. This means that a value of yield stress estimated from the intersection of two straight lines fitted to the pre-yield and post-yield sections of the compression curve in the $\varepsilon_v \cdot \ln(p')$ plot inevitably overestimates the true yield stress, even if the real soil behaviour exactly matches the assumed model. Koskinen, Karstunen & Lojander (2003) propose a more appropriate procedure, with ε_v plotted against p' (on a linear scale) and the yield point identified from the intersection of two straight lines, one a tangent to the point of shallowest gradient on the pre-yield section of the curve and one a tangent to the point of steepest gradient on the post-yield section of the curve.

The majority of tests performed to validate S-CLAY1 were restricted to triaxial tests on vertical samples. They therefore provided information relevant to only the limited form of the model represented by Eqs. 1 and 4 (a cross-anisotropic sample subjected to a co-axial cross-anisotropic stress state). A limited investigation of the generalized version of the model (Eqs. 2 and 5) is being conducted by McGinty (in press), with triaxial tests performed on samples of Bothkennar clay cut with the sample axis coinciding with a horizontal direction in the ground. Zentar, Karstunen, Wheeler & Näätänen (in press) present corresponding model simulations with S-CLAY1. Zentar, Karstunen, Wheeler & Näätänen (in press) also present S-CLAY1 simulations of a fictitious test in which the directions of the principal stresses are rotated, whilst keeping constant the values of the stress invariants p' and q . The model predicts significant plastic straining and the occurrence of substantial volumetric strains, unlike an equivalent isotropic model such as Modified Cam Clay. The predictions of the S-CLAY1 model show qualitative agreement with the results of hollow cylinder tests reported by Akagi & Saitoh (1994).

2.2 *Multilaminate Model for Clay MMC*

The Network teams at Graz and Stuttgart have worked on use of the multilaminate framework for modelling anisotropy of plastic behaviour. The models developed at Stuttgart have also incorporated either destructuration or creep/time dependency, and they are therefore described in detail in Sections 3 and 4 below. This section covers the general approach of modelling anisotropy within the multilaminate framework and the specific Multilaminate Model for Clay (MMC) developed at Graz.

The multilaminate framework was introduced for rocks and soils by Zienkiewicz & Pande (1977), Pande & Sharma (1983) and Pietruszczak & Pande (1987). Each stress integration point is associated with a large number of sampling planes at different orientations. The normal effective stress σ_n' and shear stress τ on each sampling plane are derived from the global stress tensor by a stress transformation. The stress-strain relations are then formulated locally on the planes (at the microscopic level), except for the elastic part, which is calculated at the global or macroscopic level. For an elasto-plastic model, a yield curve is defined for each sampling plane, in terms of σ_n' and τ . The global strains are obtained by numerical integration of the inelastic contribution from each sampling plane and the global elastic contribution.

When a soil element is subjected to an isotropic global stress state, the stresses on all sampling planes will be identical and therefore if the stress history is limited solely to isotropic stress states the yield curves on all planes will be of the same size. An anisotropic global stress state will, however, produce different combinations of σ'_n and τ on the different sampling planes, and hence an anisotropic stress history will result in different sizes of yield curves on the different planes. This leads to anisotropy of the yield surface presented in terms of global stresses and anisotropy of the predicted stress-strain behaviour of the soil. If the anisotropy of the global stress state subsequently applied differs from the anisotropy of the previous stress state which established the current sizes of the yield curves on the various planes, yielding will not occur simultaneously on all sampling planes. Instead, yielding will occur progressively on an increasing number of planes as the applied stress is increased. As this process occurs, the anisotropy of the yield surface defined in terms of global stresses will progressively change.

Wiltafsky, Messerklinger & Schweiger (2002) describe the Multilaminate Model for Clay (MMC) developed at Graz. In this model, the yield curve defined on each sampling plane is based on the double hardening formulation proposed by Vermeer (1978). The yield curve in the $\tau : \sigma'_n$ plane, shown in Fig. 2, consists of two parts: an elliptical volumetric hardening section (corresponding to the “cap” in Vermeer’s model) and a straight line deviatoric hardening section (corresponding to the “cone” in Vermeer’s model).

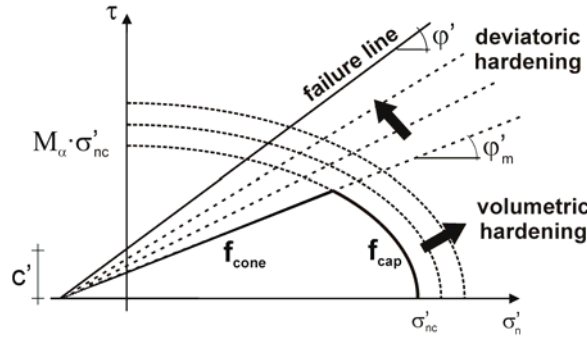


Figure 2. Multilaminate Model for Clay (MMC): yield curve on each sampling plane

The equation of the elliptical volumetric hardening cap section of the yield curve is given by:

$$f_{\text{cap}} = \left(\frac{\sigma'_n}{\sigma'_{\text{nc}}} \right)^2 + \left(\frac{\tau}{M_\alpha \sigma'_{\text{nc}}} \right)^2 - 1 = 0 \quad (6)$$

where the hardening parameter σ'_{nc} defines the current size of the yield curve (see Fig. 2) and the soil constant M_α defines the aspect ratio of the elliptical curve. M_α is not the same as the critical state stress ratio M . Hardening of the cap section of the yield curve is related solely to $d\varepsilon_{\text{n,cap}}^{\text{p}}$, the increment of plastic normal strain on the sampling plane arising from yielding on the cap, in a relationship analogous to Eq. 3:

$$d\sigma'_{\text{nc}} = \frac{v\sigma'_{\text{nc}} d\varepsilon_{\text{n,cap}}^{\text{p}}}{\lambda - \kappa} \quad (7)$$

For yielding on the volumetric hardening cap section of the curve, an associated flow rule is used to give the ratio of plastic shear strain increment $d\varepsilon_{\gamma,\text{cap}}^{\text{p}}$ to plastic normal strain increment $d\varepsilon_{\text{n,cap}}^{\text{p}}$ on the sampling plane.

The equation of the straight line deviatoric hardening section of the yield curve is given by:

$$f_{\text{cone}} = \tau - \sigma'_n \tan \phi'_m - \frac{c' \tan \phi'_m}{\tan \phi'} = 0 \quad (8)$$

where ϕ'_m is the mobilized friction angle (the hardening parameter), c' is the cohesion and ϕ' is the friction angle on the Mohr-Coulomb failure line (see Fig. 2). Hardening of this deviatoric section of the yield curve is related solely to $d\varepsilon_{\gamma, \text{cone}}^p$, the plastic shear strain on the sampling plane arising from yielding on this section of the curve, according to:

$$\tan \phi'_m = \tan \phi'_i + (\tan \phi' - \tan \phi'_i) \frac{\varepsilon_{\gamma, \text{cone}}^p}{A + \varepsilon_{\gamma, \text{cone}}^p} \quad (9)$$

where ϕ'_i is the initial value of mobilized friction angle (when $d\varepsilon_{\gamma, \text{cone}}^p=0$) and A is a soil constant. An unfortunate aspect of the hyperbolic form of the hardening relationship of Eq. 9 is that the predicted behaviour depends upon the choice of the starting point of a simulation (the point at which $\phi'_m=\phi'_i$ and $d\varepsilon_{\gamma, \text{cone}}^p=0$). Plastic flow on the deviatoric hardening section of the yield curve is governed by a non-associated flow rule (see Wiltsfsky, Messerklinger & Schweiger (2002)), using a mobilized dilation angle ψ_m , based on the stress-dilatancy theory of Rowe (1972).

Wiltsfsky, Messerklinger & Schweiger (2002) presented MMC model simulations of the experimental tests on natural Otaniemi clay samples performed at Helsinki (each test involving two loading stages, at different values of η). Similarly, Zentar, Karstunen, Wiltsfsky, Schweiger & Koskinen (2002) presented MMC simulations for the tests on natural POKO clay samples (they also presented corresponding simulations from the alternative anisotropic model S-CLAY1 and from conventional Modified Cam Clay, for comparison). In the MMC simulations, the initial anisotropic state of the soil was represented by simulating the previous application of an anisotropic stress state (corresponding to K_0 consolidation), resulting in different initial sizes of the yield curves on the various sampling planes. In the subsequent simulations with MMC, yielding occurred exclusively on the volumetric hardening cap sections of the yield curves during these tests where η was held constant during each loading stage.

The results of the MMC simulations provided a similar quality of match to the experimental data as S-CLAY1, with yield points generally well-predicted (typically much better than Modified Cam Clay) but post-yield volumetric strains often under-predicted. This under-prediction of plastic volumetric strains during some test stages was again attributed to the influence of destructuration (see Section 3 below).

In loading stages where the value of η was very different to that in the previous loading stage, MMC simulations predicted progressive yielding on the various sampling planes, and hence a gradual increase in the soil compressibility. This produced significant curvature of the post-yield compression curve, in the $\varepsilon_v \cdot \ln(p')$ plot. This matched both the behaviour predicted by S-CLAY1 (where the curvature of the post-yield compression curve resulted from rotation of the yield surface) and the behaviour observed in the experimental tests.

Neher, Cudny, Wiltsfsky & Schweiger (2002) presented MMC simulations of hollow cylinder tests reported by Akagi & Saitoh (1994) (on reconstituted clay samples) and Akagi & Yamamoto (1997) (on natural clay samples), in which the directions of the principal stresses were rotated, whilst keeping constant the values of the stress invariants p' and q . The model simulations showed significant plastic straining and development of substantial volumetric strains (similar to S-CLAY1). They provided a qualitative match to the pattern of behaviour observed in the experimental tests (a precise quantitative match was unlikely, as several model parameter values were simply guessed, in the absence of appropriate test data for the soil).

3 DESTRUCTURATION AND ANISOTROPY

Leroueil, Tavenas, Brucy, La Rochelle & Roy (1979) first introduced the term “destructuration”, to mean the post-yield disruption of the natural structure of a clay. Later, authors such as Burland (1990) defined the “structure” of a natural soil as consisting of 2 parts:

- the “fabric”, consisting of the spatial arrangement of soil particles and inter-particle contacts (this fabric can be anisotropic, as described in the previous section);
 - “bonding” between particles, which can be progressively destroyed during plastic straining.
- The term “destruction” is now often limited to the progressive damage to bonding during plastic straining, and this is the sense in which it is used here.

The presence of inter-particle bonding provides additional resistance to yielding of a soil. As a consequence, oedometer tests on natural soils generally show compression curves that plot above the “intrinsic compression line” for the reconstituted material, with the post-yield compression curve for the natural soil gradually converging with the intrinsic compression line as bonding is progressively destroyed during plastic straining. Leroueil & Vaughan (1990) showed that the influence of bonding and destruction is apparent in most natural geological materials, from soft clays to weak rocks. There are many different physical causes of real or apparent bonding in soils and rocks, but the effects on mechanical behaviour appear to be remarkably similar.

Gens & Nova (1993) presented a general framework for incorporating bonding and destruction within elasto-plastic constitutive models. In addition to the real yield surface for the natural material (with bonding) a notional “intrinsic yield surface” is introduced, to represent the size that the yield surface would be if there were no bonding. The difference in size of the real yield surface and the intrinsic yield surface (expressed either as a ratio or as a difference) is a measure of the bonding effect. Increase in size of the intrinsic yield surface is related to plastic strain increments by a conventional hardening law for unbonded (reconstituted) soil, while the reduction of bonding effect is related to plastic strain increments by a destruction law.

In recent years, a number of elasto-plastic constitutive models incorporating bonding and destruction have been published (see, for example, Lagioia & Nova (1995), Rouainia & Muir Wood (2000), Kavvas & Amorosi (2000), Baudet & Stallebrass (2001), Gajo & Muir Wood (2001) and Kavvas & Belokas (2001)). The various models differ in the precise form of destruction law applied and in the form of the underlying reference model used for the unbonded (intrinsic) material. Several of the models involve no anisotropy of large strain behaviour, which is considered essential for soft clays. Others assume that large strain anisotropy is only attributable to bonding, so that the anisotropy disappears once destruction is complete. This does not fit with experimental observations on soft clays, which show that the anisotropy of reconstituted samples subjected to an anisotropic stress history can be as great as the anisotropy of corresponding natural (bonded) samples (see, for example, the results of tests on reconstituted and natural POKO clay from Koskinen, Zentar & Karstunen (2002) and Koskinen, Karstunen & Wheeler (2002) respectively). Some of the existing models place considerable emphasis on accurate modelling of small strain behaviour. This adds considerable extra complexity, which will rarely be justified in the case of soft clays. It was therefore decided at the start of the SCMEP Network that there was still a need for a relatively simple constitutive model for soft clays, combining large strain anisotropy and destruction, but with the anisotropy not attributable solely to bonding.

Work by the Network teams at Glasgow and Helsinki on combining anisotropy and destruction has focused on adding the effects of destruction to the rotational hardening model S-CLAY1, whereas the team at Stuttgart has worked on incorporating destruction within the multilaminate framework.

3.1 Rotational hardening model with destruction S-CLAY1S

Koskinen, Karstunen & Wheeler (2002) and Zentar, Karstunen & Wheeler (2002) describe the model S-CLAY1S. This is a development of the earlier model S-CLAY1 (see Section 2.1) and is a rotational hardening elasto-plastic model incorporating the influence of bonding and destruction.

The yield surface for the natural soil (with bonding) is given by the same expression as in S-CLAY1 (Eq. 1, or the generalized version given in Eq. 2). The notional “intrinsic yield surface”,

for the equivalent unbonded soil at the same void ratio and with the same fabric, is assumed to be of the same shape and orientation as the real yield surface, but is smaller in size (Fig. 3). The size of the intrinsic yield surface is specified by a parameter p'_{mi} , and this is related to the size p'_m of the real yield surface for the natural bonded soil by a parameter x , defining the current degree of bonding:

$$p'_{mi} = (1 + x)p'_m \quad (10)$$

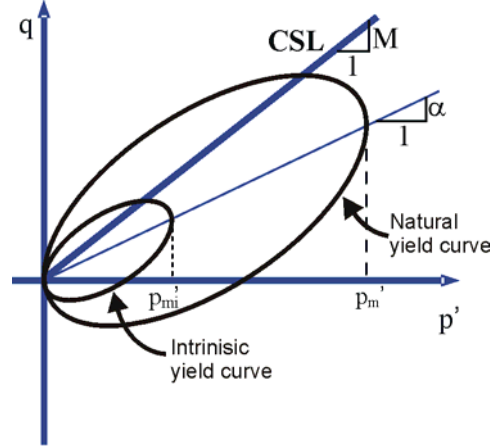


Figure 3. S-CLAY1S yield surfaces in triaxial stress space

S-CLAY1S incorporates three hardening laws. The first of these follows the logic presented by Gens and Nova (1993) and relates the change in size of the intrinsic yield surface to the plastic volumetric strain increment:

$$dp'_{mi} = \frac{v p'_{mi}}{\lambda_i - \kappa} d\varepsilon_v^p \quad (11)$$

where λ_i is the gradient of the intrinsic normal compression line (for a reconstituted soil) in the $v:\ln(p')$ plane. Eq. 11 is of the same form as the equivalent hardening law in S-CLAY1 (Eq. 3), but with p'_m replaced by p'_{mi} and λ replaced by λ_i . The rotational hardening law used in S-CLAY1S is the same as in S-CLAY1 (Eq. 4, or the generalized version of Eq. 5). The third hardening law in S-CLAY1S describes the degradation of bonding with plastic straining (the destructuration law). It is similar in form to the rotational hardening law (Eq. 4), except that both plastic volumetric strains and plastic deviatoric strains (whether positive or negative) tend to reduce the bonding parameter x towards a target value of zero:

$$dx = a \left([0 - x] |d\varepsilon_v^p| + b[0 - x] |d\varepsilon_d^p| \right) = -ax \left(|d\varepsilon_v^p| + b|d\varepsilon_d^p| \right) \quad (12)$$

where a and b are two additional soil constants. Parameter a controls the absolute rate of destructuration and parameter b controls the relative effectiveness of plastic deviatoric strains and plastic volumetric strains in destroying the bonding.

Elastic strains in S-CLAY1S are provided by the same equations as in S-CLAY1 and Modified Cam Clay (anisotropy of elastic behaviour is ignored, in the interests of simplicity). The model is completed by the assumption of an associated flow rule (as in S-CLAY1).

Combining Eqs. 10 and 11 gives:

$$d\varepsilon_v^p = \frac{(\lambda_i - \kappa) dp'_m}{vp'_m} + \frac{(\lambda_i - \kappa)(-dx)}{v(1+x)} \quad (13)$$

The increment of plastic volumetric strain predicted by S-CLAY1S can therefore be considered as consisting of two components. The first of these is related to the increase in size of the real (not the intrinsic) yield surface, and is identical to the plastic volumetric strain predicted by S-CLAY1, whereas the second component represents the additional plastic volumetric strain occurring because of destructuration. Fig. 4 illustrates the type of behaviour that would be predicted during, for example, an isotropic compression test or an oedometer test (with any change of anisotropy ignored). A reconstituted sample (with no bonding) would follow an intrinsic compression line (of gradient λ_i) in the $v:\ln(p')$ plane. In contrast, a natural sample (with initial bonding) would yield at an elevated value of effective stress, and the compression curve would then converge with the intrinsic compression line as bonding was gradually destroyed. For a natural sample, the initial gradient of the post-yield compression curve is greater than λ_i , because of the additional component of plastic volumetric strain caused by destructuration (see Eq. 13).

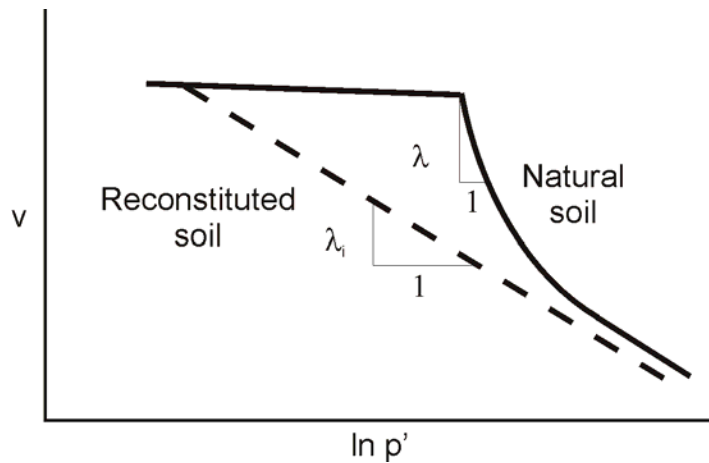


Figure 4. Predicted influence of destructuration during isotropic or oedometric loading

Koskinen, Karstunen & Wheeler (2002) suggested procedures for determining the values of the soil constants λ_i , a and b and the initial value of the bonding parameter x . The value of λ_i should be measured in oedometer tests on reconstituted samples, and this value of λ_i will often be much lower than the value of λ used in S-CLAY1 (measured in oedometer tests on natural samples). The initial value x_0 of the bonding parameter is most easily determined from the fact that the value of the sensitivity provides an estimate for $(1+x_0)$. Alternatively, x_0 can be determined from a calculation which makes use of the value of the initial void ratio e_0 (the initial value of p'_m for the natural soil and the position of the intrinsic compression line must also be known). Determination of the values of the parameters a and b requires an optimization procedure, involving model simulations of laboratory tests. This is best done by first selecting a value for the parameter a from simulations of triaxial tests involving low values of η (e.g. isotropic compression), where the shear strains are small and hence the effect of the parameter b is negligible. Then, with this optimized value of a , triaxial tests involving high values of η (where the contribution of shear strains to destructuration is important) can be simulated and used to select the most appropriate value for the parameter b .

Koskinen, Karstunen & Wheeler (2002) presented S-CLAY1S simulations of the experimental tests on natural POKO clay samples performed at Helsinki (each test involving two loading stages, at different value of η). The simulations were generally a good match to the experimental results (significantly better than the corresponding simulations with S-CLAY1). The S-CLAY1S simulations correctly predicted that the gradients of the post-yield compression curves, in $v:\ln(p')$ plots, were greater in first loading stages performed at high values of η than in first loading stages

performed at low values of η , because of the additional destructuration induced by plastic deviatoric strains. In addition, the S-CLAY1S simulations correctly predicted that the gradient of the post-yield compression curve in a second loading stage performed at a given value of η was dependent on the amount of destructuration that had occurred in the preceding first loading stage. S-CLAY1S simulations have now also been performed for the programmes of experimental tests on natural samples of Otaniemi clay, Murro clay and Vanttila clay (not yet published), and these all show excellent agreement over the full range of η values and over both loading stages of each test. Overall, therefore, it appears that the anisotropic model S-CLAY1 provides a good representation of the mechanical behaviour of reconstituted soft clays and the anisotropic model with destructuration S-CLAY1S provides a similar result for natural soft clays.

Zentar, Karstunen & Wheeler (2002) presented S-CLAY1S simulations of undrained triaxial shear tests performed on natural samples of Bothkennar clay. S-CLAY1S accurately predicted the observed stress paths and the substantial post-peak reductions of deviator stress that were observed. Of course, any numerical modelling involving this type of strain-softening behaviour would require substantial modification to the numerical implementation, because of the likelihood of strain localization.

Zentar, Karstunen & Wheeler (2003) presented S-CLAY1S simulations of a fictitious test in which the directions of the principal stresses were rotated, whilst keeping p' and q constant. The results were qualitatively similar to those described earlier for S-CLAY1.

3.2 Multilaminate model with destructuration

Cudny (2003) and Cudny & Vermeer (in press) describe the development of a multilaminate model incorporating destructuration. On each sampling plane within the multilaminate framework, the model employs the approach of Gens & Nova (1993) for modelling the influence of bonding and destructuration (a real yield curve for the bonded material and a smaller notional intrinsic yield curve for the soil in an unbonded state, with reduction in the bonding effect related to plastic strains by a destructuration law). A key feature is that the value of the bonding parameter x can be different on each sampling plane.

Fig. 5a shows the form of yield curve for the bonded soil assumed on each sampling plane, plotted in terms of the normal effective stress σ'_n and shear stress τ on the plane. The yield curve consists of two parts: a volumetric-hardening elliptical “cap” section and a non-hardening straight line section corresponding to the Mohr-Coulomb shear failure criterion. An additional soil constant β is used to control the steepness of the elliptical cap (see Fig. 5a). The size of the elliptical cap section of the curve, defined by the value of the parameter σ'_{np} (see Fig. 5a), can be different on each of the sampling planes. An associated flow rule is employed on the elliptical cap, whereas a non-associated flow rule (with a specified dilation angle ψ) is used on the Mohr-Coulomb failure line.

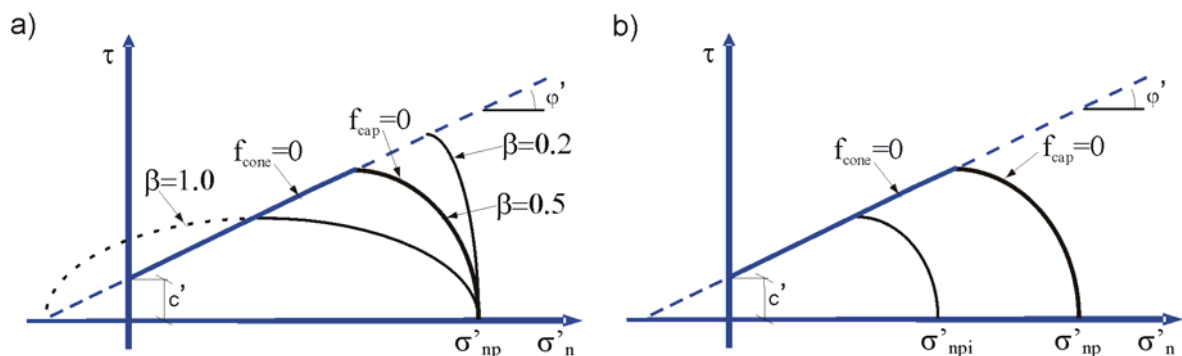


Figure 5. Multilaminate model with destructuration: a) yield curve on each sampling plane, showing influence of β ; b) intrinsic yield curve

Fig. 5b shows the form of intrinsic yield curve (for the unbonded soil) assumed on each sampling plane. The Mohr-Coulomb shear failure line is the same as for the bonded soil, but the size of the elliptical cap section is smaller than for the bonded soil. The size σ'_{npi} of the elliptical cap on the intrinsic yield curve (see Fig. 5b) is related to the size of the cap on the real yield curve by:

$$\sigma'_{npi} (1 + x) = \sigma'_{np} \quad (14)$$

where the parameter x defines the current degree of bonding on the sampling plane. The value of x can be different on each of the sampling planes.

Change in size of the cap section of the intrinsic yield curve on a given sampling plane is related to the increment of plastic normal strain on the sampling plane $d\varepsilon_n^p$:

$$d\sigma'_{npi} = \frac{\sigma'_{npi} d\varepsilon_n^p}{\lambda_i^* - \kappa^*} \quad (15)$$

where the normal compression line and elastic swelling lines for a reconstituted soil are assumed to be straight lines in a plot of volumetric strain ε_v against $\ln(p')$, with gradients λ_i^* and κ^* respectively (see Butterfield (1979)). The destructuration law employed on each sampling plane is:

$$dx = -ax \left| d\varepsilon_n^p \right| \quad (16)$$

where the parameter a controls the rate of destructuration. The implication of Equation 16 is that destructuration is currently assumed to be caused entirely by plastic normal strains on the sampling plane, with plastic shear strains having no role in the destructuration process. This appears physically unlikely, and should be compared with the destructuration law employed in S-CLAY1S (Eq. 12).

To define the initial state of anisotropy and bonding for a soil, values must be specified for σ'_{npi} (giving the size of the intrinsic yield curve) and for the bonding parameter x on each sampling plane. Cudny & Vermeer (in press) present a case where the value of σ'_{npi} is assumed to be the same on all sampling planes, but the value of x differs on the various sampling planes (anisotropy of bonding). The distribution of initial values of x over the various sampling planes makes use of a deviatoric bonding tensor (analogous to the deviatoric fabric tensor $\underline{\alpha}_d$ employed in models S-CLAY1 and S-CLAY1S; see Section 2.1). This follows the logic proposed by Pietruszczak & Pande (2001) for providing an anisotropic distribution of any mechanical property on the various sampling planes within the multilaminate framework.

Cudny & Vermeer (in press) reported that, although volumetric softening may be realistic for some heavily structured clays, this softening is difficult to employ in the multilaminate framework or to implement into a finite element program without some form of regularization. They showed that, if this softening is to be avoided, there is for each sampling plane a maximum possible value of the parameter a appearing in the destructuration law (see Eq. 16):

$$a_{\max} = \frac{1 + x_0}{x_0 (\lambda_i^* - \kappa^*)} \quad (17)$$

where x_0 is the initial value of the bonding parameter on the particular sampling plane. They also suggested that, rather than having the same value of the parameter a on all sampling planes, the value of a on each plane could be a specified ratio a_r of the maximum possible value on that particular plane.

Cudny & Vermeer (in press) present simulations, at stress point level and for a boundary value problem (an embankment), with the multilaminate model with destructuration, to show the roles of the different model parameters and to demonstrate at a qualitative level the capabilities of the model.

4 CREEP/TIME-DEPENDENCY

Creep and time-dependency of stress-strain behaviour (in addition to the time-dependent process of consolidation) are acknowledged as being particularly important for soft clays (see, for example, Bjerrum (1967), Graham, Crooks & Bell (1983), Leroueil, Kabbaj, Tavenas & Bouchard (1985), Mesri & Castro (1987) and Leroueil (2001)). Yield stresses, compression curves and undrained shear strength are all significantly dependent on the rate of straining, and if effective stresses are held constant over long time periods substantial creep strains can be observed. Constitutive models accounting for creep and time-dependency have mainly been based on elasto-viscoplasticity (e.g. Adachi & Oka (1982), Vermeer & Neher (1999) and Yin & Graham (1999)).

In the laboratory tests described in Sections 2 and 3, efforts were made to minimize the influence of creep and time-dependency, by performing all stages at fixed rates of loading or unloading. Even here, however, the effects of creep and time-dependency were clearly apparent during any rest periods at the end of loading or unloading stages, or during stages where a step increase in load was inadvertently applied for longer than intended (over a weekend or a holiday period). In practical applications, where loading rates may vary widely, or where a rapid increase of load is followed by a long period of consolidation and creep, modelling of creep and time-dependency may be of considerable importance.

Within the SCMEP Network, work on constitutive modelling of creep and time-dependency was undertaken by the teams at Stuttgart and Trondheim. In particular, the team at Stuttgart conducted validation and further development of the Soft-Soil-Creep model SSC and then went on to develop the Multilaminate-Creep model MLC (combining anisotropy and creep/time-dependency).

4.1 *Soft-Soil-Creep model SSC*

The Soft-Soil-Creep model (SSC) is described by Stolle, Bonnier & Vermeer (1997), Vermeer & Neher (1999), Neher, Wehnert & Bonnier (2001) and Neher, Vermeer & Bonnier (2001). It is an elasto-viscoplastic model, with strain increments or strain rates divided into elastic and viscoplastic components:

$$\dot{\epsilon} = \dot{\epsilon}^e + \dot{\epsilon}^{cr} \quad (18)$$

where $\dot{\epsilon}^{cr}$ is the viscoplastic or creep component of strain rate. It should be noted from Eq. 18 that there are no time-independent plastic components of strain, all plastic strains are included within the viscoplastic creep components.

For isotropic stress states, the volumetric strain rate conforms to the general statement of Eq. 18 and is given by:

$$\dot{\epsilon}_v = \kappa^* \frac{\dot{p}'}{p'} + \frac{\mu^*}{T} \left(\frac{p'}{p_p} \right)^{\frac{\lambda^* - \kappa^*}{\mu^*}} \quad (19)$$

The first term on the right hand side of Eq. 19 is the elastic volumetric strain rate, which is directly proportional to the rate of increase of mean effective stress p' (elastic swelling lines are assumed to be straight lines, of gradient κ^* , in a plot of volumetric strain against $\ln(p')$). The second term is the viscoplastic or creep component of volumetric strain rate. μ^* is the modified creep index, related to the conventional creep index C_α by:

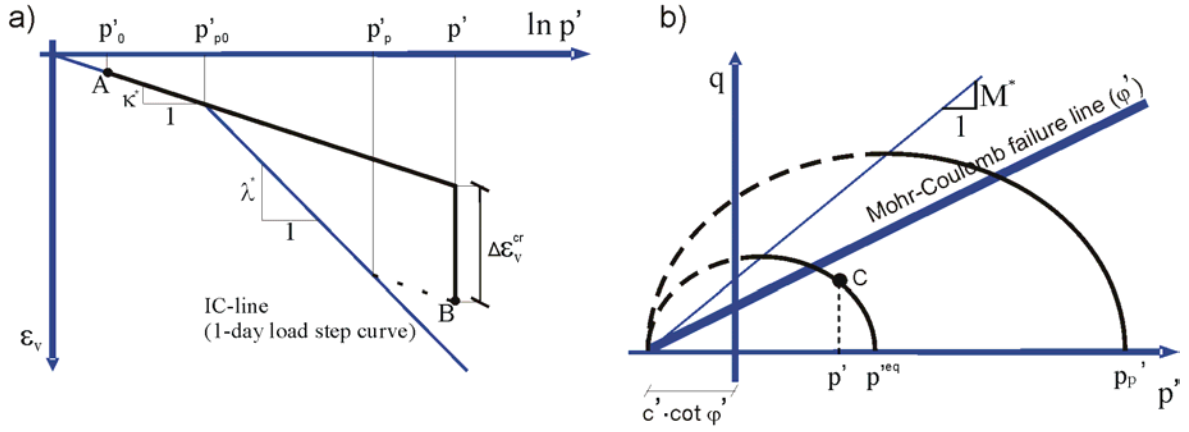


Figure 6. Soft-Soil-Creep (SSC): a) isotropic stress states b) triaxial stress states

$$\mu^* = \frac{C_\alpha}{v \ln 10} \quad (20)$$

This is analogous to the relationship between the modified compression index λ^* and the conventional compression index C_c :

$$\lambda^* = \frac{\lambda}{v} = \frac{C_c}{v \ln 10} \quad (21)$$

T in Eq. 19 is a reference time (typically taken as 1 day), and p'_p is defined by reference to the so-called IC-line. This IC-line is the “post-yield” compression curve corresponding to a test where the load is increased step-wise and each load step is maintained for a constant period T (i.e. typically the conventional 1-day step loading compression curve). The IC-line has a gradient λ^* in the $\varepsilon_v:\ln(p')$ plot (see Fig. 6a). p'_p is defined from the intersection of the IC-line and an elastic line drawn through the current state of the soil in the $\varepsilon_v:\ln(p')$ plane (see Fig. 6a) i.e. it is the value of p' at a point on the IC-line corresponding to the same creep strain as has actually occurred.

Fig. 6a shows a situation where loading commences at point A, at a mean effective stress p'_0 , and the stress is then increased, either instantaneously or over a period of time, to a value p' . Some time after the load application the soil state plots as point B. The current value of p'_p , for use in Eq. 19, can then be derived from the magnitude of creep strain $\Delta\varepsilon_v^{cr}$ that has occurred since point A (see Fig. 6a):

$$p'_p = p'_{p0} \exp\left(\frac{\Delta\varepsilon_v^{cr}}{\lambda^* - \kappa^*}\right) \quad (22)$$

where p'_{p0} is the initial value of p'_p (the intersection of the IC-line and an elastic line drawn through point A, see Fig. 6a). Eq. 22 shows that p'_p increases with time, as creep strains occur.

Inspection of Eq. 19 shows that creep strain rates depend upon the current state of the soil in the $\varepsilon_v:\ln(p')$ plot relative to the IC-line, through the ratio p'/p'_p , which is greater than 1 for states that plot above the IC-line and less than 1 for states that plot below the line. The exponent $(\lambda^* - \kappa^*)/\mu^*$ in Eq. 19 typically has a value of at least 20 (Mesri & Castro (1987)), so creep strain rates change very dramatically with the ratio p'/p'_p . Creep strain rates are high if the soil state plots on the IC-line (this would conventionally be viewed as a normally consolidated state). Creep strain rates increase exponentially with the distance from the IC-line if the soil state plots above the line.

Conversely, creep strain rates decrease exponentially with the distance from the IC-line if the soil state plots below the line (this would conventionally be viewed as an overconsolidated state).

To extend the model to triaxial stress states, an elliptical cap surface is drawn through the current stress point C in the $q:p'$ plane (see Fig. 6b). A soil constant M^* (which is not the same as the critical state stress ratio M) defines the aspect ratio of the ellipse. The size of the cap surface through the current stress point is defined by a parameter p'^{eq} (see Fig. 6b). Also shown in Fig. 6b is a second elliptical cap surface with a size p'_p , where p'_p is the point on the isotropic IC-line corresponding to the same creep strain as has actually occurred. This viscoplastic cap surface of size p'_p increases in size with time, as creep strains occur, according to Eq. 22. The ratio p'/p'_p controlling the creep strain rate term in Eq. 19 is now replaced by p'^{eq}/p'_p . The volumetric strain rate $\dot{\epsilon}_v$ is then given by:

$$\dot{\epsilon}_v = \kappa^* \frac{\dot{p}'}{p'} + \frac{\mu^*}{T} \left(\frac{p'^{\text{eq}}}{p'_p} \right)^{\frac{\lambda^* - \kappa^*}{\mu^*}} \quad (23)$$

An associated flow rule is assumed on the cap surface, to provide the magnitude of the deviatoric creep strain rate.

For general stress states, the strain rate tensor $\dot{\underline{\epsilon}}$ is given by:

$$\dot{\underline{\epsilon}} = \underline{\underline{D}}_e^{-1} \underline{\underline{\dot{\sigma}'}} + \frac{\mu^*}{T} \frac{\partial p'^{\text{eq}}}{\partial p'} \left(\frac{p'^{\text{eq}}}{p'_p} \right)^{\frac{\lambda^* - \kappa^*}{\mu^*}} \frac{\partial p'^{\text{eq}}}{\partial \underline{\underline{\sigma}'}} \quad (24)$$

where $\underline{\underline{D}}_e$ is the fourth order elastic stress-strain tensor.

The model is completed by a non-hardening Mohr-Coulomb failure line (see Fig. 6b), with plastic strains (rather than time-dependent creep strains) occurring on this failure line.

The SSC model is able to represent many experimentally-observed time-dependent features of soft clay behaviour. Apparent yield stresses (during oedometric, isotropic or triaxial loading) are all predicted to be dependent on the applied rate of loading or straining. Under the application of constant effective stresses, creep strains are predicted to increase in a fashion which gradually approaches a linear rate of increase with the logarithm of time. In addition, undrained shear strength is predicted to increase with increasing loading rate.

4.2 Multilaminar Creep model MLC

Neher, Vermeer & Bonnier (2001) and Neher, Cudny, Wiltafsky and Schweiger (2002) describe the Multilaminar Creep model (MLC) developed at Stuttgart. This model combines anisotropy (represented by the multilaminar framework) with creep/time-dependency. Modelling of viscoplastic creep behaviour on the sampling planes of the multilaminar framework follows the logic of the Soft-Soil-Creep model (SSC) described in the previous section.

The local stress state on a sampling plane can be expressed in terms of the normal effective stress σ'_n and shear stress τ on the plane, see point C in Fig. 7. An elliptical cap curve, of size $\sigma'_n{}^{\text{eq}}$, can be drawn through the current stress point (see Fig. 7). This can be related to a viscoplastic cap curve, of the same shape, but of size σ'_{np} . The size of this viscoplastic cap curve increases with time, as creep strains occur on the sampling plane, according to:

$$\sigma'_{np} = \sigma'_{np0} \exp \left(\frac{\Delta \epsilon_n^{\text{cr}}}{\lambda^* - \kappa^*} \right) \quad (25)$$

where $\Delta \varepsilon_n^{cr}$ is the creep component of normal strain on the sampling plane that has occurred since the start of the simulation (when the size of the viscoplastic cap curve was defined by $\sigma'_{np} = \sigma'_{np0}$).

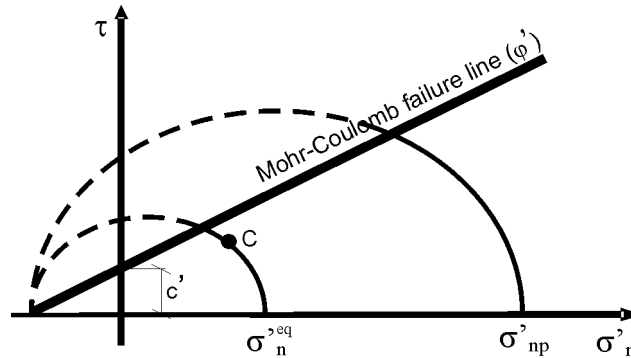


Figure 7. Multilaminare Creep model (MLC): viscoplastic cap curve and Mohr-Coulomb failure line on each sampling plane

The creep normal strain rate on the sampling plane is given, by analogy with Eq. 23, as:

$$\dot{\varepsilon}_n^{cr} = \frac{\mu^*}{T} \left(\frac{\sigma_n^{req}}{\sigma'_{np}} \right)^{\frac{\lambda^* - \kappa^*}{\mu^*}} \quad (26)$$

An associated flow rule on the cap curve is used to calculate the creep shear strain rate on the sampling plane $\dot{\varepsilon}_v^{cr}$. Behaviour on the plane is completed by a Mohr-Coulomb failure line in the $\tau : \sigma'_n$ plane (see Fig. 7), with plastic strains (rather than creep strains) occurring on this failure line. Finally, global strains are obtained by numerical integration of the inelastic contribution from each sampling plane (consisting of creeps strains related to the viscoplastic cap and any plastic strains from yielding on the failure surface) and then the addition of the global elastic strains.

Neher, Cudny, Wiltafsky & Schweiger (2002) presented MLC simulations of hollow cylinder tests involving rotation of the principal stress directions whilst the stress invariants p' and q were held constant. The model predictions were very similar to those from the Multilaminare Model for Clay (MMC) developed at Graz (see Section 2.2) and were generally a good match to the hollow cylinder test results reported by Akagi & Saitoh (1994) and Akagi & Yamamoto (1997).

5 CONCLUSIONS

The two alternative methods of representing anisotropy of plastic behaviour (elasto-plastic models with a rotational component of hardening, as represented by S-CLAY1, or the multilaminare approach, as represented by the Multilaminare Model for Clays MMC) both appear to provide a realistic representation of experimentally-observed yield behaviour of soft clays. Each of the two approaches has now been combined with modelling of the influence of bonding and destructuration, to form the rotational hardening model with destructuration S-CLAY1S and the Multilaminare Model with Destructuration respectively. For situations where creep strains and time-dependency can be ignored, S-CLAY1 or MMC provide accurate modelling of the behaviour of reconstituted soft clays, and S-CLAY1S or the Multilaminare Model with Destructuration provide accurate modelling of natural soft clays (where destructuration is important).

Modelling of creep and time-dependency of stress-strain behaviour has been achieved within the elasto-viscoplastic Soft-Soil-Creep model (SSC). This has been combined with modelling of anisotropy in the Multilaminare Creep model (MLC).

The Multilaminate Model for Clay (MMC), the Multilaminate Model with Deconstruction, the Soft-Soil-Creep model (SSC) and the Multilaminate Creep model (MLC) have all been implemented in the PLAXIS finite element program. The rotational hardening models S-CLAY1 and S-CLAY1S have been implemented in the finite element code SAGE Crisp and are currently being implemented in PLAXIS. The various constitutive models have been employed in the numerical analysis of both fictitious benchmark boundary value problems and real case histories.

Future objectives of the research teams within the SCMEP Network include:

- To combine creep/time-dependency with the rotational hardening approach to modelling anisotropy, by developing a viscoplastic creep version of S-CLAY1.
- To combine anisotropy, deconstruction and creep/time-dependency within a single constitutive model, employing either the multilaminate approach or the rotational hardening approach.
- To conduct further experimental validation of the various constitutive models and to refine the models where necessary. Ideally, experimental validation should include extension to generalized stress states by, for example, hollow cylinder testing.
- To demonstrate further the enhanced capabilities provided by the various constitutive and numerical modelling developments, to disseminate the improved capabilities to other researchers and to practitioners, and to encourage more widespread practical application.
- To apply the enhanced modelling capabilities to the study of ground improvement techniques in soft clays.

ACKNOWLEDGEMENTS

The following individuals have contributed to the research reported in this paper: Marcin Cudny, Lars Grande, Frantisek Havel, Minna Karstunen, Mirva Koskinen, Harald Krenn, Matti Lojander, Kevin McGinty, Sophie Messerklinger, Anu Nääänen, Heiko Neher, Helmut Schweiger, Pieter Vermeer, Simon Wheeler, Christoph Wiltafsky and Rachid Zentar. Apologies to any individuals inadvertently omitted from this list, or individuals whose work has been mis-represented in any way.

The research was carried out as part of a Research Training Network on “Soft Clay Modelling for Engineering Practice” (SCMEP), supported by the European Community through the programme “Improving the Human Research Potential and the Socio-Economic Knowledge Base” (Grant HPRN-CT-1999-00049). Various other funding sources have supported individual components of the research.

REFERENCES

- Adachi, T. & Oka, F. 1982. Constitutive equations for normally consolidated clays based on elasto-viscoplasticity. *Soils and Foundations* 22:57-70.
- Akagi, H. & Saitoh, J. 1994. Dilatancy characteristics of clayey soil under principal stress axes rotation. In S. Shibuya, T. Mitachi & S. Miura (ed.), *Proc. Int. Symp. on Prefailure Deformation Characteristics of Geomaterials, Sapporo*, Vol. 1: 311-314. A.A. Balkema.
- Akagi, H. & Yamamoto, H. 1997. Stress-dilatancy relation of undisturbed clay under principal axes rotation. In A. Asaoko, T. Adachi & F. Oka (ed.), *Deformation and Progressive Failure in Geomechanics, Proc. IS-Nagoya '97*: 211-216. Elsevier.
- Banerjee, P.K. & Yousif, N.B. 1986. A plasticity model for the mechanical behaviour of anisotropically consolidated clay. *International Journal for Numerical and Analytical Methods in Geomechanics* 10: 521-541.
- Baudet, B.A. & Stallebrass, S.E. 2001. Modelling the deconstruction of soft natural clays. In Desai et al. (ed.), *Proc. 10th Int. Conf. on Computer Methods and Advances in Geomechanics, Tucson* : 297-301. A.A. Balkema.
- Bjerrum, L. 1967. 7th Rankine Lecture : Engineering geology of Norwegian normally-consolidated marine clays as related to settlements of buildings. *Géotechnique* 17(1): 81-118.
- Burland, J.B. 1990. 30th Rankine Lecture: On the compressibility and shear strength of natural clays. *Géotechnique* 40(3): 327-378.

- Butterfield, R. 1979. A natural compression law for soils (an advance on e-log p'). *Géotechnique* 29(4): 469-480.
- Cudny, M. 2003. Simple multi-laminate model for soft soils incorporating structural anisotropy and destructuration. In P.A. Vermeer, H.F. Schweiger, M. Karstunen & M. Cudny (ed.), *Proc. Int. Workshop on Geotechnics of Soft Soils : Theory and Practice, Noordwijkerhout*. VGE.
- Cudny, M. & Vermeer, P.A. (in press). On the modelling of anisotropy and destructuration of soft clays within the multi-laminate framework. Submitted to *Computers and Geotechnics*.
- Dafalias, Y.F. 1987. Anisotropic critical state clay plasticity model. In *Proc. 2nd Int. Conf. on Constitutive Laws for Engineering Materials, Tucson*. Vol. 1: 513-521. Elsevier.
- Davies, M.C.R. & Newson, T.A. 1993. A critical state constitutive model for anisotropic soils. In G.T. Housley & A.N. Schofield (ed.), *Predictive Soil Mechanics: Proc. Wroth Memorial Symposium*: 219-229. Thomas Telford.
- Diaz-Rodriguez, J.A., Leroueil, S. & Aleman, J.D. 1992. Yielding of Mexico City clay and other natural clays. *Journal of Geotechnical Engineering* 118 (7): 981-995.
- Gajo, A. & Muir Wood, D. 2001. A new approach to anisotropic bounding surface plasticity : general formulation and simulations of natural and reconstituted clay behaviour. *International Journal for Numerical and Analytical Methods in Geomechanics* 25: 207-241.
- Gens, A. & Nova, R. 1993. Conceptual bases for a constitutive model for bonded soils and weak rocks. In A. Anagnostopoulos, F. Schlosser, N. Kalteziotis & R. Frank (ed.), *Proc. Int. Symp. on Geomechanical Engineering of Hard Soils and Soft Rocks, Athens*: 485-494. A.A. Balkema.
- Graham, J., Crooks, J.H.A. & Bell, A.L. 1983. Time effects on stress-strain behaviour of natural soft clays. *Géotechnique* 33(3): 327-340.
- Karstunen, M. & Wheeler, S.J. 2002. Discussion of : Voyiadjis, G.Z. and Song, C.R. 2000. Finite strain, anisotropic Modified Cam Clay model with plastic spin. 1: Theory. *Journal of Engineering Mechanics, ASCE* 128: 497-498.
- Kavvas, M. & Amorosi, A. 2000. A constitutive model for structured soils. *Géotechnique* 50(3): 263-274.
- Korhonen, K.-H. & Lojander, M. 1987. Yielding of Perno clay. In *Proc. 2nd Int. Conf. on Constitutive Laws for Engineering Materials, Tucson*. Vol. 2: 1249-1255. Elsevier.
- Koskinen, M., Karstunen, M. & Lojander, M. 2003. Yielding of "ideal" and natural anisotropic clays. In P.A. Vermeer, H.F. Schweiger, M. Karstunen & M. Cudny (ed.), *Proc. Int. Workshop on Geotechnics of Soft Soils : Theory and Practice, Noordwijkerhout*. VGE.
- Koskinen, M., Karstunen, M. & Wheeler, S.J. 2002. Modelling destructuration and anisotropy of a natural soft clay. In P. Mestat (ed.), *Proc. 5th European Conf. on Numerical Methods in Geotechnical Engineering (NUMGE 2002), Paris*: 11-20. Presses de l'ENPC.
- Koskinen, M., Zentar, R. & Karstunen, M. 2002. Anisotropy of reconstituted POKO clay. In G.N. Pande & S. Pietruszczak (ed.), *Proc. 8th Int. Symp. on Numerical Models in Geomechanics (NUMOG VIII), Rome*: 99-105. A.A. Balkema.
- Lagioia, R. & Nova, R. 1995. An experimental and theoretical study of the behaviour of a calcarenite in triaxial compression. *Géotechnique* 45(4): 633-648.
- Leroueil, S. 2001. Some fundamental aspects of soft clay behaviour and practical implications. In C.F. Lee, C.K. Lau, C.W.W. Ng, A.K.L. Kwong, P.L.R. Pang, J.-H. Yin & Z.Q. Yue (ed.), *Proc. 3rd Int. Conf. on Soft Soil Engineering, Hong Kong*: 37-53. A.A. Balkema.
- Leroueil, S., Kabbaj, M., Tavenas, F. & Bouchard, R. 1985. Stress-strain-strain rate relation for the compressibility of sensitive natural clays. *Géotechnique* 35(2): 159-180.
- Leroueil, S., Tavenas, F., Brucy, F., La Rochelle, P. & Roy, M. 1979. Behaviour of destructured natural clays. *Journal of Geotechnical Engineerig Div. ASCE* 105(6): 759-778.
- Leroueil, S. & Vaughan, P.R. 1990. The general and congruent effects of structure in natural soils and weak rocks. *Géotechnique* 40 (3): 467-488
- McGinty, K. (in press). The stress-strain behaviour of Bothkennar clay. PhD thesis, University of Glasgow, UK.
- McGinty, K., Karstunen, M. & Wheeler, S.J. 2001. Modelling the stress-strain behaviour of Bothkennar clay. In C.F. Lee, C.K. Lau, C.W.W. Ng, A.K.L. Kwong, P.L.R. Pang, J.-H. Yin & Z.Q. Yue (ed.), *Proc. 3rd Int. Conf. on Soft Soil Engineering, Hong Kong*: 263-268. A.A. Balkema.
- Mesri, G. & Castro, A. 1987. The C_α/C_c concept and K_0 during secondary compression. *Journal of Geotechnical Engineerig, ASCE*, 113(3): 230-247.

- Näätänen, A. & Lojander, M. 2000. Modelling of anisotropy of Finnish clays. In *Proc. 7th Finnish Symp. on Mechanics, Tampere*: 589-598. Tampere University of Technology.
- Näätänen, A., Wheeler, S.J., Karstunen, M. & Lojander, M. 1999. Experimental investigation of an anisotropic hardening model for soft clays. In M.Jamiolkowski, R. Lancellotta & D. Lo Presti (ed.), *Proc. 2nd Int. Symp. on Pre-failure Deformation Characteristics of Geomaterials, Torino*, Vol. 1: 541-548. A.A. Balkema.
- Neher, H.P., Cudny, M., Wiltafsky, C. & Schweiger, H.F. 2002. Modelling principal stress rotation effects with multilaminate type constitutive models for clay. In G.N. Pande & S. Pietruszczak (ed.), *Proc. 8th Int. Symposium on Numerical Models in Geomechanics (NUMOG VIII), Rome*: 41-47. A.A. Balkema.
- Neher, H.P., Vermeer, P.A. & Bonnier, P.G. 2001. Strain-rate effects in soft soils, modelling and application. In C.F. Lee, C.K. Lau, C.W.W. Ng, A.K.L. Kwong, P.L.R. Pang, J.-H. Yin & Z.Q. Yue (ed.), *Proc. 3rd Int. Conf. on Soft Soil Engineerig, Hong Kong*: 361-367. A.A. Balkema.
- Neher, H.P., Wehnert, M. & Bonnier, P.G. 2001. An evaluation of soil models based on trial embankments. In Desai et al. (ed.), *Proc. 10th Int. Conf. on Computer Methods and Advances in Geomechanics, Tucson*: 373-378. A.A. Balkema.
- Pande, G.N. & Sharma, K.G. 1983. Multilaminate model of clays - a numerical evaluation of the influence of rotation of principal stress axes. *International Journal for Numerical and Analytical Methods in Geomechanics*, Vol. 7: 397-418.
- Pestana, J.M. & Whittle, A.J. 1999. Formulation of a unified constitutive model for clays and sands. *International Journal for Numerical and Analytical Methods in Geomechanics*, Vol. 23: 1215-1243.
- Pietruszczak, S. & Pande, G.N. 1987. Multi-laminate framework of soil models-plasticity formulation. *International Journal for Numerical and Analytical Methods in Geomechanics*, Vol. 11(6): 651-658.
- Pietruszczak, S. & Pande, G.N. 2001. Description of soil anisotropy based on multi-laminate framework. *International Journal for Numerical and Analytical Methods in Geomechanics*, Vol. 25: 197-206.
- Roscoe, K.H. & Burland, J.B. 1968. On the generalized stress-strain behaviour of 'wet' clay. In *Engineerig Plasticity*. 553-609. Cambridge University Press.
- Rouainia, M. & Muir Wood, D. 2000. A kinematic hardening constitutive model for natural clays with loss of structure. *Géotechnique*, Vol. 50(2): 153-164.
- Rowe, P.W. 1972. Theoretical meaning and observed values of deformation parameters for soil. *Proc. Roscoe Memorial Symposium*. 143-194. Cambridge University Press.
- Stolle, D.F.E., Bonnier, P.G. & Vermeer, P.A. 1997. A soft soil model and experiences with two integration schemes. In S. Pietruszczak & G.N. Pande (ed.), *Proc. 6th Int. Symp. on Numerical Models in Geomechanics (NUMOG VI), Montreal*: 123-128, A.A. Balkema.
- Vermeer, P.A. 1978. A double hardening model for sands. *Géotechnique* 28(4): 413-433.
- Vermeer, P.A. & Neher, H.P. 1999. A soft soil model that accounts for creep. In R.B.J. Brinkgreve (ed.), *Proc. Int. Symp. Beyond 2000 in Computational Geotechnics : 10 Years of Plaxis International* : 249-261. A.A. Balkema..
- Wheeler, S.J. 1997. A rotational hardening elasto-plastic model for clays. In *Proc. 14th Int. Conf. on Soil Mechanics and Foundation Engineering, Hamburg, Vol. 1* : 431-434. A.A. Balkema.
- Wheeler, S.J., Karstunen, M. & Näätänen, A. 1999. Anisotropic hardening model for normally consolidated soft clay. In G.N. Pande, S. Pietruszczak & H.F. Schweiger (ed.), *Proc. 7th Int. Symp. on Numerical Models in Geomechanics (NUMOG VII), Graz* : 33-40. A.A. Balkema.
- Wheeler, S.J., Näätänen, A., Karstunen, M. & Lojander, M. 2003. An anisotropic elastoplastic model for soft clays. *Canadian Geotechnical Journal* 40: 403-418.
- Whittle, A.J. & Kavvas, M.J. 1994. Formulation of MIT-E3 constitutive model for overconsolidated clays. *Journal of Geotechnical Engineering* 120(1): 173-198.
- Wiltafsky, C., Messerklinger, S. & Schweiger, H.F. 2002. An advanced multilaminate model for clay. In G.N. Pande & S. Pietruszczak (ed.), *Proc. 8th Int. Symp. on Numerical Models in Geomechanics (NUMOG VIII), Rome*: 67-73. A.A. Balkema.
- Yi, J.-H. & Graham, J. 1999. Elastic viscoplastic modelling of the time-dependent stress-strain behaviour of soils. *Canadian Geotechnical Journal* 36: 736-745.
- Yu, Y. & Axelsson, K. 1994. Constitutive modelling of Swedish cohesive soils accounting for anisotropy. *Proc. 8th Int. Conf. on Computer Methods and Advances in Geomechanics*: 737-743. A.A. Balkema.

- Zentar, R., Karstunen, M. & Wheeler, S.J. 2002. Influence of anisotropy and destructuration on undrained shearing of natural clays. In P. Mestat (ed.), *Proc. 5th European Conf. on Numerical Methods in Geotechnical Engineering (NUMGE 2002)*, Paris: 21-26. Presses de l'ENPC.
- Zentar, R., Karstunen, M. & Wheeler, S.J. 2003. Modelling principal stress rotation of structural clays. In P.A. Vermeer, H.F. Schweiger, M. Karstunen & M. Cudny (ed.), *Proc. Int. Workshop on Geotechnics of Soft Soils: Theory and Practice, Noordwijkerhout*. VGE.
- Zentar, R., Karstunen, M., Wheeler, S.J. & Näätänen, A. (in press). Modelling plastic anisotropy and rotation of principal stresses with S-CLAY1 model. Submitted to *International Journal for Numerical and Analytical Methods in Geomechanics*.
- Zentar, R., Karstunen, M., Wiltafsky, C., Schweiger, H.F. & Koskinen, M. 2002. Comparison of two approaches for modelling anisotropy of soft clays. In G.N. Pande & S. Pietruszczak (ed.), *Proc. 8th Int. Symp. on Numerical Models in Geomechanics (NUMOG VIII)*, Rome: 115-121. A.A. Balkema.
- Zienkiewicz, O.C. & Pande, G.N. 1977. Time-dependent multilaminar model of rocks - a numerical study of deformation and failure of rock masses. *International Journal for Numerical and Analytical Methods in Geomechanics* 1(3): 219-247.